2021-11-16

Percolation threshold and effective properties of CNTs-reinforced two-phase composite materials

Fang, Y

http://hdl.handle.net/10026.1/18375

10.1016/j.mtcomm.2021.102977
Materials Today Communications
Elsevier BV

Article reference: MTCOMM_102977
Journal: Materials Today Communications
Received: 17 Aug 2021
Article revised: 3 Nov 2021
Article accepted: 5 Nov 2021
DOI: 10.1016/j.mtcomm.2021.102977

Percolation threshold and effective properties of CNTs-reinforced two-phase composite materials

Yuan Fang[1], Shouwang Hu[2], Long-yuan Li[3*], Sung-Hwan Jang[4]

1) Guangdong Provincial Key Laboratory of Durability for Marine Civil Engineering, Shenzhen University, Shenzhen 518060, P R China (yuanfang@szu.edu.cn)

2) School of Environment and Civil Engineering, Dongguan University of Technology, Dongguan 523808, P R China (shouwang.hu@dgut.edu.cn)

3) School of Engineering, Computing and Mathematics, University of Plymouth, Plymouth, Devon PL4 8AA, UK (long-yuan.li@plymouth.ac.uk)

4) School of Engineering, Hanyang University ERICA, Ansan, Gyeonggi-do 15588, South Korea (sj2527@hanyang.ac.kr)

Abstract – In this paper an analytical prediction model is developed to determine the percolation threshold and effective properties of carbon nanotubes reinforced two-phase composite materials. The model considers the effect of not only volume fraction but also aspect ratio and mixed pattern of fibres in the composites. It is shown that the effect of fibres on the effective properties of the composites can be characterised in terms of three different zones, namely non-percolated zone, partially percolated zone, and fully percolated zone. The formulations for determining percolation threshold and effective properties of the composites in the three different zones are derived. The model is validated by using available experimental data to demonstrate its appropriateness and reliability.

Keywords: Composites; CNTs; Percolation threshold; Effective properties; Aspect ratio.

* Corresponding author

1. Introduction

A composite material is a combination of two or more materials with different physical and chemical properties. The bulk properties of the composite material can be significantly different from those of any of its individual constituents. By choosing an appropriate combination of constitutive materials, manufacturers can produce properties that closely fit the requirements for a particular structure with a particular purpose. Nowadays composite materials have been used in many fields such as aerospace, architecture, automotive, energy, infrastructure, marine, military, and sports and recreation.

It is well known that for a matrix-composite material its thermal, electrical and mechanical properties, often named as effective properties, are dependent on the properties of the matrix and fillers or inclusions forming the composite, the volume fraction and aspect ratio of the fillers, and the way how the fillers are dispersed and distributed in the matrix [1,2]. It has been widely reported that, the effective property of a composite, such as its electrical conductivity, changes slightly when the volume fraction of fillers is very small, but sharply when the volume fraction of fillers reaches to a certain narrow range [3]. This phenomenon is characterised as the percolation [4], which describes the connectivity of fillers within the matrix and its effect on the macroscale properties of the composite. In literature various percolation models have been developed to describe the effective properties of fibre-reinforced composite materials in which a sharp insulator–conductor transition is typically observed with increasing filler fraction [5]. For instance, Wu et al. [6] carried out an experimental investigation on the conductivity of asphalt concrete containing conductive fillers. Ma and Gao [7] developed a 3-D Monte Carlo model for predicting electrical conductivity of polymer matrix composites filled with conductive curved fibres. It was found that the curliness largely influenced the percolation threshold, and the more curved the fibre, the higher the threshold. Savchenko and Ionov [8] used experimental methods to investigate the electrical and thermal properties of binary systems consisting of stearine, expanded and fine-crystalline graphite. It was demonstrated that the percolation threshold depended on the aspect ratio of the electro-conducting filler. Dubnikova et al. [9] examined the effects of multi-walled carbon nanotubes (CNTs) dimensions and surface modification on the morphology, mechanical reinforcement, and electrical properties of polypropylene-based composites prepared by melt mixing. It was demonstrated that the nanocomposites based on long large diameter CNTs had the lowest percolation threshold. Martone et al. [10] examined the effect of dispersed multi-walled CNTs on the bending modulus of their reinforced epoxy systems. It was shown that reinforcement efficiency was characterised by two limiting behaviours whose transition region coincides with the development of a percolative network of CNTs. Lonjon et al. [11] provided a comparative study on the percolation threshold of two polymer composites; one was reinforced with nanowires and the other was with spherical nanoparticles. Feng and Jiang [12] presented a mixed micromechanics model to predict the overall electrical conductivity of CNTs-reinforced polymer composites. It was shown that the size of CNTs had a significant effect on the percolation threshold of nanocomposites. Wang et al. [13] examined the effect of aspect ratio on the electrical conductivity and crystallization kinetics of semi-crystalline polystyrene composites filled with graphene nano-sheets. Kim et al. [14] presented an analytical homogenization approach for composites containing multiple heterogeneities with conductive coated layers to predict the percolation threshold of polymer composites containing randomly oriented ellipsoidal inclusions. Yang et al. [15] proposed a micromechanics-based model to investigate the effect of CNTs agglomeration on the electrical conductivity and percolation threshold of nanocomposites. Wu et al. [16] investigated the thermal and electrical properties of polypropylene composites with dense small-sized multi-walled CNTs network located within loosened large-sized expanded graphite network. It was suggested that the formation of double percolated filler network could effectively reduce the interface thermal resistance. Taherian [17] presented an analytical formula to predict the electrical conductivity of composites reinforced by conductive fillers. The work employed a sigmoidal equation to describe the relationship between electrical conductivity and filler volume fraction. The results showed that the aspect ratio and size of fillers were the most important factors affecting percolation threshold. Nilsson et al. [18] developed three different simulation models based on finite element, percolation threshold and electrical networks, respectively for predicting electrical conductivity and percolation threshold of field-grading polymer composites. Chiu et al. [19] investigated the rheological and electrical properties of syndiotactic polystyrene composites filled with graphene nano-sheets and CNTs to reveal the effect of filler concentration, in which percolation scaling laws were applied to the magnitudes of storage modulus and electrical conductivity to determine the threshold concentration and corresponding exponent function. Lu et al. [20] proposed a numerical modelling framework to evaluate the effective electric conductivity in polymer composites reinforced with graphene sheets, taking into account the electrical tunnelling effect. Fang et al. [21] presented an analytical study on the electrical conductivity of composites whose constitutive materials have distinct electrical properties. Formulations were derived for determining percolation threshold and electrical conductivity of composites with considering aspect ratio effect. Zare and Rhee [22] examined the effects of filler network and interfacial shear strength on the mechanical properties of CNTs-reinforced nanocomposites. Xu et al [23] proposed a theoretical framework for predicting excluded volume and percolation threshold of soft interphase and effective conductivity of carbon fibrous composites. Recently, Tang et al. [24] presented an analytical model to predict the percolation threshold and electrical conductivity of CNTs-reinforced composites by taking into account the effects of CNTs waviness and dispersion. It was indicated that high electrical conductivity could be achieved for composites with CNTs of high conductivity, large aspect ratio, perfect dispersion state and low degree of waviness. Chang et al. [25] developed a simulation model to examine the effect of deformation on the percolation threshold and electrical conductivity of composites with fillers, in which the percolating filler networks were modelled as an equivalent electrical circuit consisting of tunnelling and intrinsic resistances. Xu et al. [26] performed a numerical simulation to estimate the percolation threshold of 3-D porous media interacted by anisotropic-shaped pores and cracks and their effects on the thermal conductivity and elastic modulus of the media. Chang et al. [27] developed a numerical model on the structural evolution of conductive polymer composites subjected to mechanical loading action. The model was used to examine the effect of deformation on the percolation threshold and effective electrical conductivity of composites with fillers. Fang et al. [28] presented an analytical model which can be used to examine the effect of mechanical strains on the percolation threshold and effective electrical conductivity of CNTs-reinforced two-phase composites.

CNTs have excellent thermal, electrical, and mechanical properties. The use of CNTs as inclusions in polymer matrix can improve the thermal, electrical, and mechanical properties of the polymer-based composites and produce functionally graded smart materials and/or smart sensors. To achieve the purpose of the improvement and function required, however, it is necessary to know the percolation threshold of CNTs for a given CNTs-reinforced polymer composite. The literature survey described above shows that there have been numerous experimental and numerical investigations but limited prediction models available on the percolation threshold to elucidate how the effective properties vary with CNTs volume fraction. In this paper, an analytical model is developed to predict the percolation threshold and effective properties of fibre reinforced two-phase composite materials. The model considers the effect of volume fraction, aspect ratio, and mixed pattern of fibres in the composites. Compared to existing analytical models published in literature, the present model has the following new features. Firstly, the percolation threshold is derived based on randomly dispersed fibres which are characterised by three identical ellipsoids perpendicularly placed along with three axes in Cartesian coordinate system. Secondly, the effective properties are calculated based on three different zones, namely non-percolated zone, partially percolated zone, and fully percolated zone. These three zones are characterised mathematically based on the aspect ratio and volume fraction of inclusions in the composite. Thirdly, the prediction formulas derived can be applied to all of the three zones. Fourthly, to demonstrate the present model, comparisons between the present model and existing experimental data are also provided for composites with different constitutive materials for various different volume fractions of inclusions in different zones.

2. Effective properties of two-phase composite materials

In a two-phase matrix composite material, the matrix and fillers can be treated as the homogeneous medium and inclusions in the composite, respectively. The effective properties of the two-phase composite such as the thermal conductivity, electrical conductivity, diffusion coefficient, and elastic modulus, can be estimated using the Maxwell model [29] if the inclusions are small spheres and perfectly enclosed by the matrix,

$$P_{el} = P_2 \frac{(P_1+2P_2)+2V_1(P_1-P_2)}{(P_1+2P_2)-V_1(P_1-P_2)} \tag{1}$$

where P_{el} is the effective property of the composite, V_1 is the volume fraction of the inclusions, P_1 and P_2 are the properties of the inclusions and matrix material, respectively. Conversely, if we assume the matrix material is made by small spheres that are perfectly enclosed by the inclusions, then a different version of Eq.(1) can be obtained as follows,

$$P_{eu} = P_1 \frac{(P_2+2P_1)+2(1-V_1)(P_2-P_1)}{(P_2+2P_1)-(1-V_1)(P_2-P_1)} \tag{2}$$

where P_{eu} is also the effective property of the composite. For the case of $P_1>P_2$ Eqs.(1) and (2) give the lower- and upper-bounds of the effective property of the two-phase composite. Fig.1 graphically plots the variation of P_{el} and P_{eu} with V_1. The percolation threshold of the Maxwell model is V_p=1 when Eq.(1) is used and V_p=0 when Eq.(2) is used. Eqs.(1) and (2) represent the two extreme cases of mixes in the two-phase composite. In reality, however, neither the medium nor inclusions would be perfectly covered by the medium or inclusions. In general, Eq.(1) is more suitable for the composite with small volume fraction of inclusions; whereas Eq.(2) is more apposite for the composite with large volume fraction of inclusions. Therefore, with the increase in volume fraction of inclusions, the effective property of the composite will have a "jump" from the lower-bound curve to the upper-bound curve. The volume fraction corresponding to the "jumping" point is characterised as the percolation threshold of the composite. By assuming the medium and inclusions are perfectly symmetric in the geometry of the composite, Bruggeman [30] and Landauer [31] proposed independently an effective medium approximation for calculating the effective property of the two-phase composite,

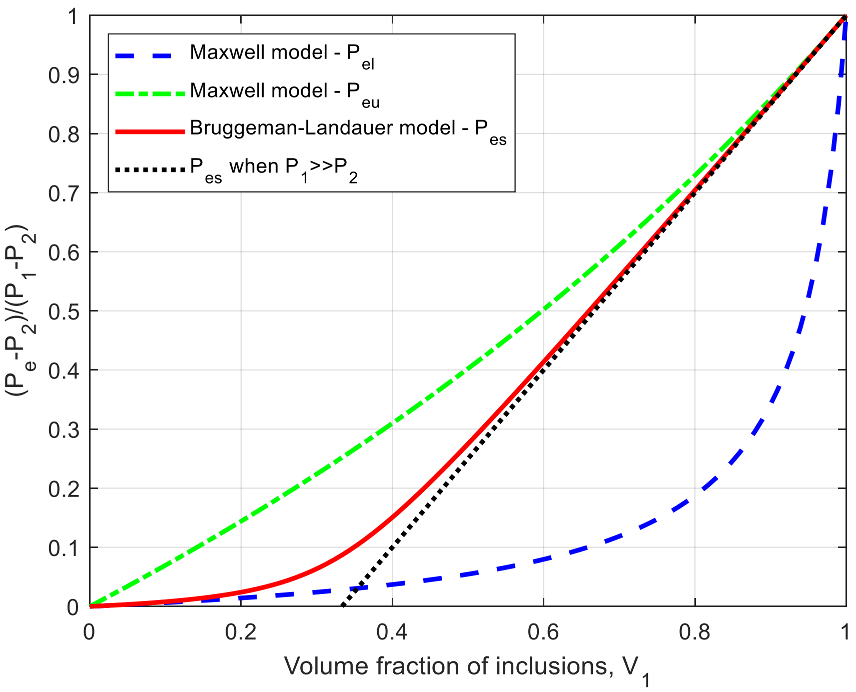

Fig.1 Effective property in Maxwell and Bruggeman-Landauer models (P_1=50P_2).

$$\frac{(P_{es}-P_1)}{(2P_{es}+P_1)}V_1 + \frac{(P_{es}-P_2)}{(2P_{es}+P_2)}(1-V_1) = 0 \quad (3)$$

where P_{es} is the effective property of the two-phase composite. The variation of P_{es} with V_1 described by Eq.(3) is also plotted in Fig.1. It can be seen from the figure that P_{es} almost coincides with P_{el} for small volume fraction of inclusions and to P_{eu} for large volume fraction of inclusions. In the middle region of $0.2 \leq V_1 \leq 0.8$ P_{es} drives away from the lower-bound curve and gradually approaches to the upper-bound curve. For the case of $P_1 >> P_2$, Eq.(3) can be simplified as,

$$P_{es} = \begin{cases} P_2 & V_1 \leq 1/3 \\ P_2 + \frac{(3V_1-1)}{2}(P_1 - P_2) & V_1 > 1/3 \end{cases} \quad (4)$$

This indicates that the percolation threshold of the effective medium approximation is about 1/3, as shown by the black dot line in Fig.1. Eq.(3) illustrates how the volume fraction of inclusions influences P_{es}, leading it to vary from lower-bound curve to upper-bound curve.

Here, however, it should be noted that Eq.(3) was developed for spherical inclusions in which the aspect ratio of inclusions is one. For many fibre-reinforced composites the aspect ratio of inclusions is much greater than one [3,21] and the corresponding percolation threshold would be very low. To take account for the effects of aspect ratio and percolation threshold of inclusions on the effective properties of fibre-reinforced composites, we have to know the relationship between the percolation threshold and aspect ratio of inclusions and find out where the effective property leaves from the lower-bound curve and how quickly it reaches to the upper-bound curve.

3. Percolation threshold of fibre-reinforced two-phase composite materials

For a given two-phase composite material, if the aspect ratio and mixed pattern of inclusions in the composite are known then the percolation threshold and corresponding effective properties of the composite can be calculated analytically or numerically. For example, Pan et al. [2] presented an analytical expression of percolation threshold for transversely orthotropic composites containing randomly oriented ellipsoidal inclusions. Fang et al. [21] proposed an analytical expression of percolation threshold for isotropic composites containing prismatic inclusions equally distributed in three axial directions. Both models showed that the percolation threshold decreases with increased aspect ratio of inclusions. However, the downside of these models is that when the aspect ratio tends to one the percolation threshold also attends to one. To improve the model proposed by Fang et al. [21], here we consider a unit cube as the representative volume element (RVE) of the fibre reinforced two-phase composite material. The volume of fibres in the RVE is represented by three identical ellipsoids perpendicularly placed along with three axes as shown in Fig.2a, which can be expressed as follows,

$$\Omega_{in}(\lambda, a) = \frac{4\pi a^3}{\sqrt{(1+\lambda^2)^3}}\left(\frac{3-4\sqrt{2}}{3} + \frac{\sqrt{(1+\lambda^2)^3}-1}{\lambda^2}\right) \tag{5}$$

where Ω_{in} is the volume of fibres in the RVE, λ is the aspect ratio of fibres, and a is the longer semi-axis of the ellipsoids. The detail of the derivation of Eq.(5) is given in the Appendix. At the state that the fibres reach to percolation, the inner ellipsoids should be inscribed in the outer cube as shown in Fig.2b. Mathematically this condition is expressed by $2a=1$. Thus, the threshold volume fraction of fibres, or the percolation threshold of the fibre-reinforced two-phase composite material, can be expressed as follows,

$$V_p(\lambda) = \frac{\pi}{2\sqrt{(1+\lambda^2)^3}}\left(\frac{3-4\sqrt{2}}{3} + \frac{\sqrt{(1+\lambda^2)^3}-1}{\lambda^2}\right) \tag{6}$$

Note that if $\lambda=1$ Eq.(6) gives $V_p=\pi/6$, indicating that the percolation threshold for the spherical inclusions in the present model is slightly greater than 0.5. The effective property of the composite depends not only on the volume fraction of fibres but also on the mixed pattern of fibres in the composite. The volume fraction may also affect the mixed pattern. Three different mixed patterns are assumed in the present approach in terms of the volume fraction of fibres. Case one is when the volume fraction of fibres is less than its percolation threshold V_p. In this case the mixed pattern is assumed as a three-layer sphere as shown in Fig.2c, in which the core part represents the matrix enclosed by the outer sphere inscribing the ellipsoids with partial volume fraction V_{m1}, the middle layer represents the fibres with volume fraction V_{in1}, and the outer layer represents the rest matrix with partial volume fraction V_{m2}. These three volume fractions are defined as follows,

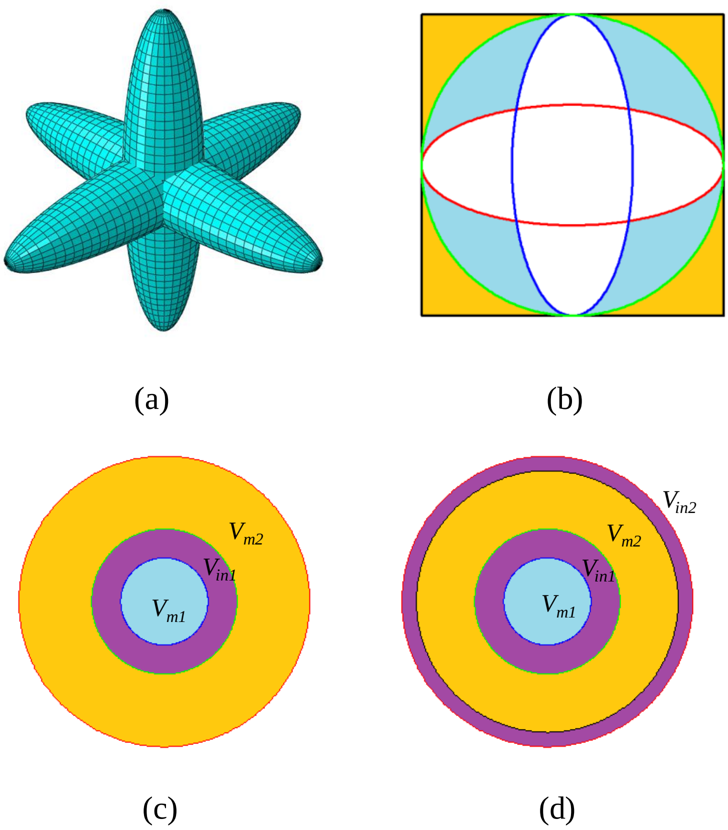

Fig.2. (a) Three ellipsoids placed along with three axes. (b) Definitions of volumes of fibres and matrix in composite. Mixed patterns (c) before and (d) after percolation.

Case 1: $V_{in} \leq V_p$

$$V_{in1} = V_{in} = \frac{4\pi a^3}{\sqrt{(1+\lambda^2)^3}}\left(\frac{3-4\sqrt{2}}{3} + \frac{\sqrt{(1+\lambda^2)^3}-1}{\lambda^2}\right) \tag{7}$$

$$V_{m1} = \frac{4\pi a^3}{3} - V_{in} \tag{8}$$

$$V_{m2} = 1 - \frac{4\pi a^3}{3} \tag{9}$$

where V_{in} is the volume fraction of fibres in the composite. For given V_{in} and λ, *a* can be calculated from Eq.(7). For the two-layer sphere with core part (matrix) plus the middle layer (fibres) we can use Eq.(2) by letting $P_1=P_{in}$, $P_2=P_m$, $V_1=V_{in1}/(V_{in1}+V_{m1})$ to obtain its effective property,

$$P_e^{(0)} = P_{in}\frac{(P_m+2P_{in})+\frac{2V_{m1}}{V_{in1}+V_{m1}}(P_m-P_{in})}{(P_m+2P_{in})-\frac{V_{m1}}{V_{in1}+V_{m1}}(P_m-P_{in})} \tag{10}$$

where P_{in} and P_m is the property of the fibres and matrix, respectively. For the three-layer sphere we can use Eq.(1) by letting $P_1=P_e^{(0)}$, $P_2=P_m$, $V_1=(V_{in1}+V_{m1})/(V_{in1}+V_{m1}+V_{m2})$ to obtain its effective property,

$$P_e^{(1)} = P_m\frac{\left(P_e^{(0)}+2P_m\right)+\frac{2(V_{in1}+V_{m1})}{V_{in1}+V_{m1}++V_{m2}}\left(P_e^{(0)}-P_m\right)}{\left(P_e^{(0)}+2P_m\right)-\frac{V_{in1}+V_{m1}}{V_{in1}+V_{m1}++V_{m2}}\left(P_e^{(0)}-P_m\right)} \tag{11}$$

where $P_e^{(1)}$ represents the effective property of the three-layer sphere with the mixed pattern as shown in Fig.2c, respectively.

Case two is when the volume fraction of fibres is greater than its percolation threshold V_p. In this case the mixed pattern is assumed as a four-layer sphere as shown in Fig.2d, in which the core part represents the matrix enclosed by the outer sphere of unit diameter inscribing the ellipsoids (see Fig.2b) with partial volume fraction $V_{m1}=\pi/6-V_p$, the inner middle layer represents the part of the fibres with percolation volume fraction V_p (see Fig.2b), the outer middle layer represents the rest matrix with partial volume fraction V_{m2}, and the outer layer represents the rest fibres with partial volume fraction V_{in2}. These four volume fractions are defined as follows,

Case 2: $V_p \leq V_{in} \leq 1-\pi/6+V_p$

$$V_{in1} = V_p \tag{12}$$

$$V_{in2} = V_{in} - V_p \tag{13}$$

$$V_{m1} = \frac{\pi}{6} - V_p \tag{14}$$

$$V_{m2} = 1 - V_{m1} - V_{in} \tag{15}$$

The effective property of the four-layer sphere can be calculated as follows,

$$P_e^{(2)} = P_{in}\frac{\left(P_e^{(1)}+2P_{in}\right)+\frac{2(V_{in1}+V_{m1}+V_{m2})}{V_{in1}+V_{in2}+V_{m1}++V_{m2}}\left(P_e^{(1)}-P_{in}\right)}{\left(P_e^{(1)}+2P_{in}\right)-\frac{V_{in1}+V_{m1}+V_{m2}}{V_{in1}+V_{in2}+V_{m1}++V_{m2}}\left(P_e^{(1)}-P_{in}\right)} \tag{16}$$

where $P_e^{(1)}$ is defined by Eq.(11). The concept of using a recursive formula for Eqs.(10), (11) and (16) is illustrated in [21,32] and thus is not discussed further here. Finally, case three is when the volume fraction of fibres is greater than ($1-\pi/6+V_p$), in which case the matrix V_{m2} in the outer middle layer of the four-layer sphere disappears and thus the effective property of the composite reaches to its upper-bound, that is,

Case 3: $1-\pi/6+V_p \leq V_{in}$

$$P_e^{(3)} = P_{eu} \tag{17}$$

Physically, $P_e^{(3)}$ represents the effective property of the sphere where the matrix is completely enclosed by the fibres. Eqs.(11), (16) and (17) represent the non-percolated, partially percolated, and fully percolated composite, respectively. The effective property calculated using these equations reflect the effects of volume fraction, aspect ratio, and pattern of distribution and dispersion of fibres in the composite. The effective property of the composite is calculated differently in different zones. The definition of the three zones is governed by the percolation threshold. Fig.3 shows a comparison of the percolation threshold obtained from various different models including analytical [2,21] and numerical [26,33,34,35] models. It can be seen from the figure that the percolation thresholds given from different models are almost identical when the aspect ratio is greater than 10. In the region of 4>λ>8, Fang's model is slightly closer to those predicted by numerical models; whereas the present model performs reasonable well for all range of the aspect ratio. Fig.4 plots the variation of the effective property with the volume fraction of fibres for different aspect ratios. The figure demonstrates that, the effective property increases slowly in the non-percolated zone; then quickly in the partially percolated zone, and finally it merges to the upper-bound curve in the fully percolated zone. The aspect ratio of fibres has a significant effect on the positions where the effective property starts to jump and where it lands to the upper-bound curve. However, the aspect ratio has no influence on the effective property after it reaches to the upper-bound.

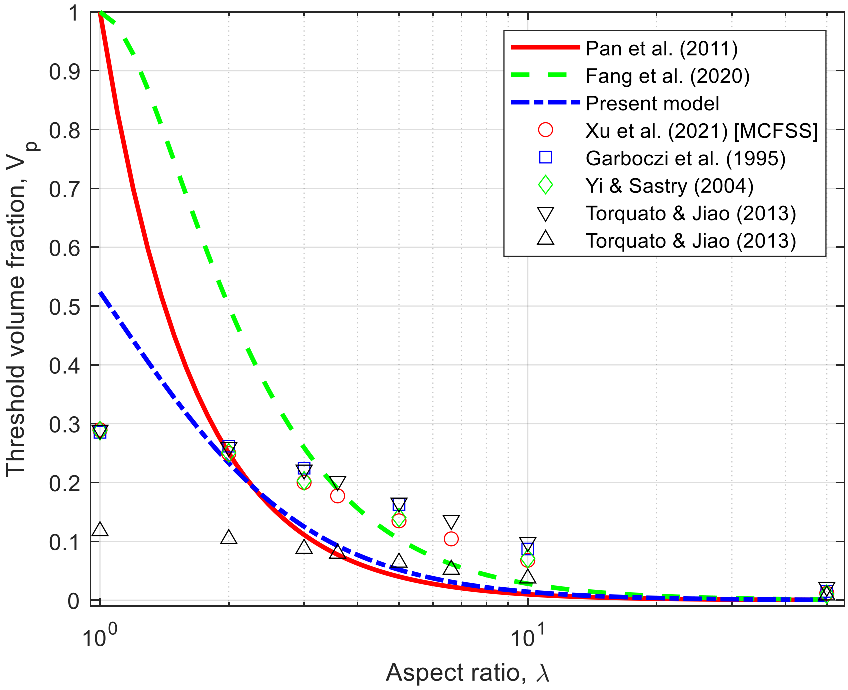

Fig.3 Variation of threshold volume fraction with aspect ratio of inclusions at percolation.

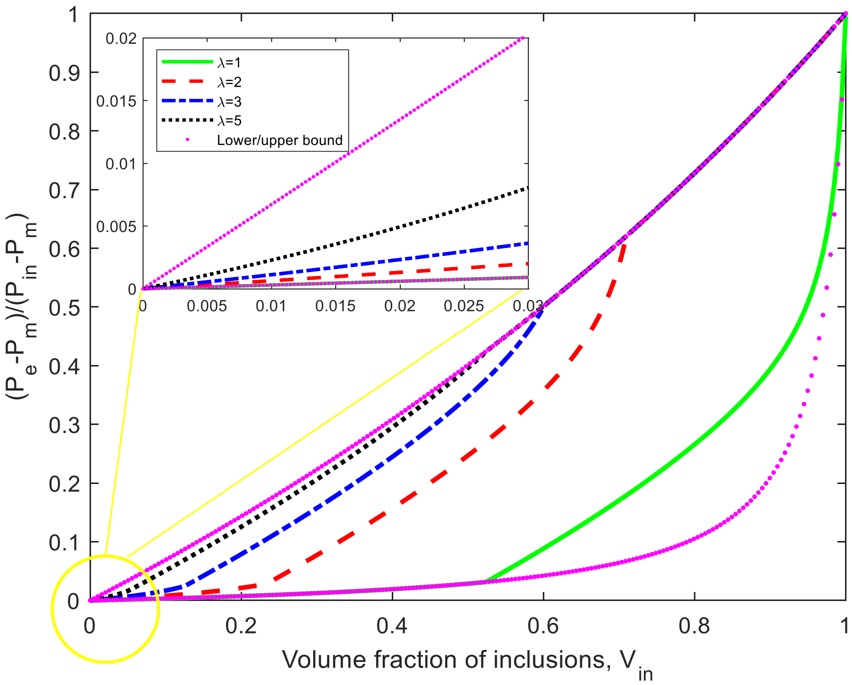

Fig.4 Variation of effective property with volume fraction of inclusions for different aspect ratios (P_1=100P_2).

4. Validation of model with experimental results

To validate the present model, experimental data published in literature are used for three different composite materials. The first one is the multi-walled CNTs-reinforced cement paste for which the experimental data of effective electrical conductivity were reported in [36]. From the simulation it is found that the percolation threshold of the CNTs-reinforced cement is about V_p=4.83%. Thus the experimental data obtained for V_{in}<1.01% are all in the non-percolated zone. In the calculation, the value of P_m (electrical conductivity of cement paste) is obtained directly from the test, whereas the value of P_{in} (electrical conductivity of CNTs) is reduced after taking into account the tunnelling effect of CNTs. Fig.5 shows the comparison between the model prediction and test data. It can be seen from the figure that the effective electrical conductivities predicted in the model and measured in the experiment are reasonably close and have very similar variation attendance.

The second one is the moisture-enhanced cement paste for which the experimental data of effective electrical conductivity were reported in [36]. The percolation threshold of the moisture-enhanced cement is assumed to be V_p=0.5, which means that the pores in the cement are very close to spherical shape. The experimental data obtained from the test for V_{in}<0.4 thus are all in non-percolated zone. In the calculation, both the values of P_m (electrical conductivity of cement paste) and P_{in} (electrical conductivity of moisture) are obtained directly from the test. Fig.6 shows the comparison between the model prediction and test data. It can be seen from the figure that there is very good agreement between the predicted and measured effective electrical conductivities.

The third one is the A4 multi-walled CNTs-reinforced epoxy composite. The experimental data of effective electrical conductivity were reported in [37]. The percolation threshold of the CNTs-reinforced epoxy composite is found to be about V_p=0.12%, which is much lower than that of the CNTs-reinforced cement paste. The experimental data obtained from the tests for $V_{in}\leq$3.0% thus covers all of three zones. In the calculation, the value of P_m (electrical conductivity of epoxy) is obtained directly from the test, whereas the value of P_{in} (electrical conductivity of CNTs) is reduced after taking into account the tunnelling effect of CNTs. Fig.7 shows the comparison between the model prediction and test data. Excellent agreement between the prediction and test data is demonstrated.

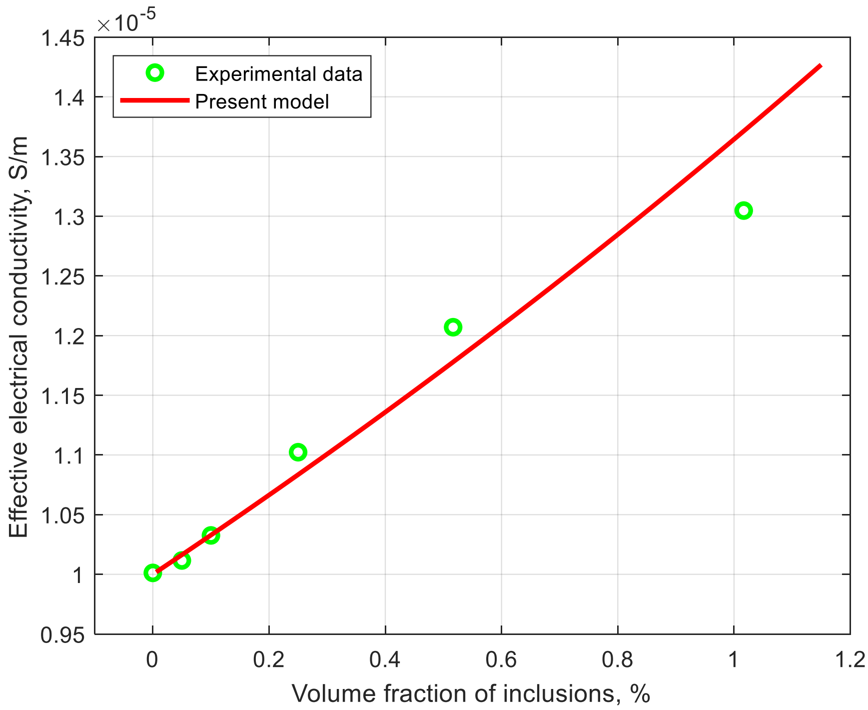

Fig.5 Comparison of effective electrical conductivity of CNT-reinforced fresh mortar between prediction and experiment (V_p=4.83%, P_m=1.0x10^{-5} S/m, P_{in}=5.0 S/m).

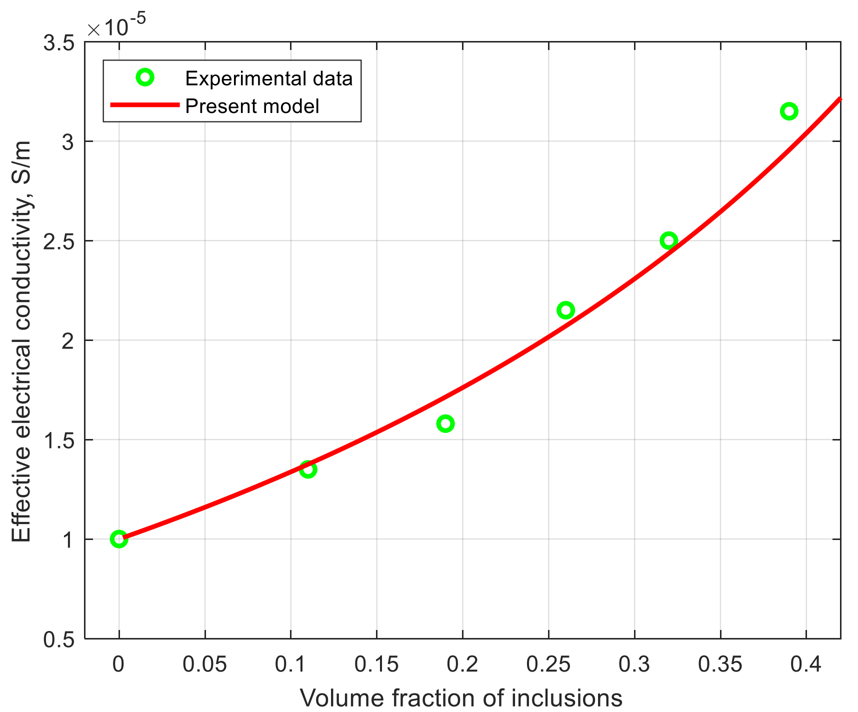

Fig.6 Comparison of effective electrical conductivity of moisture-enhanced cement between prediction and experiment (V_p=0.5, P_m=1.0x10^{-5} S/m, P_{in}=1.0x10^{-3} S/m).

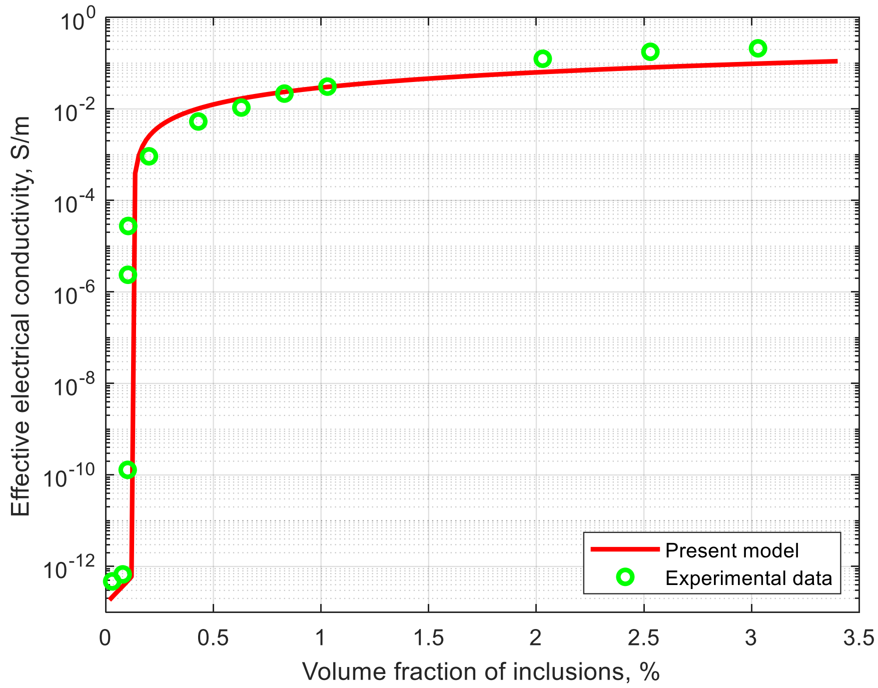

Fig.7 Comparison of effective electrical conductivity of CNT-reinforced epoxy composite between prediction and experiment (V_p=0.12%, P_m=1.5x10^{-13} S/m, P_{in}=5.0 S/m).

5. Conclusions

This paper has presented an analytical model for determining percolation threshold and calculating the effective properties of fibre reinforced two-phase composite materials. The model has been validated by using experimental data published in literature. From the results obtained we have the following conclusions.

- The percolation threshold of a two-phase composite can be determined by using a unit length RVE cube inscribed by three equal ellipsoids placed perpendicularly along three axes. The volume fraction of the ellipsoids inside the RVE represents the percolation threshold of the composite.
- According to the percolation threshold, the effect of the volume fraction of inclusions on the effective properties of the composite can be characterised in terms of non-

percolated zone, partially percolated zone, and fully percolated zone, respectively. These three zones have different mixed patterns and thus the ways used to calculate the effective properties are also different.

- In the non-percolated zone, the inclusions infold a small part of matrix but themselves are completely implanted in the matrix. The change of volume fraction of inclusions in this zone leads to a limited change of effective properties of the composite due to the fact that the inclusions are isolated by the matrix.
- In the partially percolated zone, part of inclusions become connective although some of inclusions are still implanted in the matrix. With the increase of volume fraction of inclusions, more inclusions become connective, leading to a big change in the effective properties of the composite.
- In the fully percolated zone, all inclusions become connective and the matrix is completely enclosed by the connected inclusions. Thus the effective properties in this zone can be calculated by using the upper-bound formula of the two-phase composite. After it reaches to the upper-bound, the aspect ratio no longer has influence on the effective property of the composite.

Acknowledgments – The work presented in the paper was supported by the National Natural Science Foundation of China (grant No. 52078300 and 52008107), Guangdong Basic and Applied Basic Research Foundation in China (grant No. 2019A1515111032), and the Ministry of Land, Infrastructure and Transport of South Korea (grant No. 21CTAP-C151808-03).

Declaration of interests - The authors declare that they have no known competing financial interests or personal relationships that could have appeared to influence the work reported in this paper.

References

[1] M.H. Jomaa, K. Masenelli-Varlot, L. Seveyrat, L. Lebrun, M.C.D. Jawhar, E. Beyou, J.Y. Cavaillé, Investigation of elastic, electrical and electromechanical properties of polyurethane/grafted carbon nanotubes nanocomposites, Composites Science and Technology 121 (2015) 1-8. https://doi.org/10.1016/j.compscitech.2015.10.019.

[2] Y. Pan, G.J. Weng, S.A. Meguid, W.S. Bao, Z.H. Zhu, A.M.S. Hamouda, Percolation threshold and electrical conductivity of a two-phase composite containing randomly oriented ellipsoidal inclusions, Journal of Applied Physics 110 (2011) 123715. https://doi.org/10.1063/1.3671675.

[3] A.A. Snarskii, M. Shamonin, P. Yuskevich, Effective medium theory for the elastic properties of composite materials with various percolation thresholds, Materials 13(5) (2020) 1243. https://doi.org/10.3390/ma13051243.

[4] M. Sahini, M. Sahimi, Applications of Percolation Theory, CRC Press, London (1994).

[5] V.I. Irzhak, Percolation threshold in polymer nanocomposites, Colloid Journal 83 (2021) 64–69. https://doi.org/10.1134/S1061933X21010063.

[6] S. Wu, L. Mo, Z. Shui, Z. Chen, Investigation of the conductivity of asphalt concrete containing conductive fillers, Carbon 43(7) (2005) 1358-1363. https://doi.org/10.1016/j.carbon.2004.12.033.

[7] H.M. Ma, X.L. Gao, A three-dimensional Monte Carlo model for electrically conductive polymer matrix composites filled with curved fibres, Polymer 49(19) (2008) 4230-4238. DOI:10.1016/j.polymer.2008.07.034.

[8] D.V. Savchenko, S.G. Ionov, Physical properties of carbon composite materials with low percolation threshold, Journal of Physics and Chemistry of Solids 71(4) (2010) 548-550. https://doi.org/10.1016/j.jpcs.2009.12.033.

[9] I. Dubnikova, E. Kuvardina, V. Krasheninnikov, S. Lomakin, I. Tchmutin, S. Kuznetsov, The effect of multi-walled carbon nanotube dimensions on the morphology, mechanical, and electrical properties of melt mixed polypropylene-based composites, Journal of Applied Polymer Science 117(1) (2010) 259-272. https://doi.org/10.1002/app.31979.
[10] A. Martone, C. Formicola, M. Giordano, M. Zarrelli, Reinforcement efficiency of multi-walled carbon nanotube/epoxy nano-composites, Composites Science and Technology 70(7) (2010) 1154-1160. https://doi.org/10.1016/j.compscitech.2010.03.001.
[11] A. Lonjon, P. Demont, E. Dantras, C. Lacabanne, Low filled conductive P(VDF-TrFE) composites: Influence of silver particles aspect ratio on percolation threshold from spheres to nanowires, Journal of Non-Crystalline Solids 358(23) (2012) 3074-3078. DOI:10.1016/J.JNONCRYSOL.2012.09.006.
[12] C. Feng, L. Jiang, Micromechanics modelling of the electrical conductivity of carbon nanotube (CNT)-polymer nanocomposites, Composites Part A: Applied Science and Manufacturing 47(1) (2013) 143-149. https://doi.org/10.1016/j.compositesa.2012.12.008.
[13] C. Wang, Y.C. Chiu, C.L. Huang, Electrical percolation and crystallization kinetics of semi-crystalline polystyrene composites filled with graphene nanosheets, Materials Chemistry and Physics 164 (2015) 206-213. https://doi.org/10.1016/j.matchemphys.2015.08.046.
[14] S.Y. Kim, Y.J. Noh, J. Yu, Prediction and experimental validation of electrical percolation by applying a modified micromechanics model considering multiple heterogeneous inclusions, Composites Science and Technology 106 (2015) 156-162. https://doi.org/10.1016/j.compscitech.2014.11.015.
[15] B.J. Yang, K.J. Cho, G.M. Kim, H.K. Lee, Effect of CNT agglomeration on the electrical conductivity and percolation threshold of nanocomposites: A micromechanics-based

approach, Computer Modelling in Engineering and Sciences 103(5) (2015) 343-365. doi:10.3970/cmes.2014.103.343.

[16] K. Wu, Y. Xue, W. Yang, S. Chai, F. Chen, Q. Fu, Largely enhanced thermal and electrical conductivity via constructing double percolated filler network in polypropylene/ expanded graphite – Multi-wall carbon nanotubes ternary composites, Composites Science and Technology 130 (2016) 28-35. DOI:10.1016/j.compscitech.2016.04.034.

[17] R. Taherian, Experimental and analytical model for the electrical conductivity of polymer-based nanocomposites, Composites Science and Technology 123 (2016) 17-31. https://doi.org/10.1016/j.compscitech.2015.11.029.

[18] F. Nilsson, J. Krückel, D.W. Schubert, F. Chen, M. Unge, U.W. Gedde, M.S. Hedenqvist, Simulating the effective electric conductivity of polymer composites with high aspect ratio fillers, Composites Science and Technology 132 (2016) 16-23. https://doi.org/10.1016/j.compscitech.2016.06.008.

[19] Y.C. Chiu, C.L. Huang, C. Wang, Rheological and conductivity percolations of syndiotactic polystyrene composites filled with graphene nanosheets and carbon nanotubes: A comparative study, Composites Science and Technology 134 (2016) 153-160. https://doi.org/10.1016/j.compscitech.2016.08.016.

[20] X. Lu, J. Yvonnet, F. Detrez, J. Bai, Multiscale modelling of nonlinear electric conductivity in graphene-reinforced nanocomposites taking into account tunnelling effect, Journal of Computational Physics 337 (2017) 116-131. https://doi.org/10.1016/j.jcp.2017.01.063.

[21] Y. Fang, L.Y. Li, S.H. Jang, Calculation of electrical conductivity of self-sensing carbon nanotube composites, Composites Part B: Engineering 199 (2020) 108314. https://doi.org/10.1016/j.compositesb.2020.108314.

[22] Y. Zare, K.Y. Rhee, Modelling the effects of filler network and interfacial shear strength on the mechanical properties of carbon nanotube-reinforced nanocomposites, The Journal of The Minerals, Metals & Materials Society (JOM) 72(6) (2020) 2184-2190. DOI:10.1007/s11837-020-04083-x.

[23] W. Xu, P. Lan, Y. Jiang, D. Lei, H. Yang, Insights into excluded volume and percolation of soft interphase and conductivity of carbon fibrous composites with core-shell networks, Carbon 161 (2020) 392-402. https://doi.org/10.1016/j.carbon.2020.01.083.

[24] Z.H. Tang, Y.Q. Li, P. Huang, Y.Q. Fu, N. Hu, S.Y. Fu, A new analytical model for predicting the electrical conductivity of carbon nanotube nanocomposites, Composites Communications 23 (2021) 100577. https://doi.org/10.1016/j.coco.2020.100577.

[25] E. Chang, A. Ameli, A.R. Alian, L.H. Mark, K. Yu, S. Wang, C.B. Park, Percolation mechanism and effective conductivity of mechanically deformed 3-dimensional composite networks: Computational modelling and experimental verification, Composites Part B: Engineering 207 (2021) 108552. https://doi.org/10.1016/j.compositesb.2020.108552.

[26] W. Xu, Y. Zhang, J. Jiang, Z. Liu, Y. Jiao, Thermal conductivity and elastic modulus of 3D porous/fractured media considering percolation, International Journal of Engineering Science 161 (2021) 103456. https://doi.org/10.1016/j.ijengsci.2021.103456.

[27] E. Chang, A. Ameli, A.R. Alian, L.H. Mark, K. Yu, S. Wang, C.B. Park, Percolation mechanism and effective conductivity of mechanically deformed 3-dimensional composite networks: Computational modelling and experimental verification, Composites Part B: Engineering 207 (2021) 108552. https://doi.org/10.1016/j.compositesb.2020.108552.

[28] Y. Fang, L.Y. Li, S.H. Jang, Piezoresistive modelling of CNTs reinforced composites under mechanical loadings, Composites Science and Technology 208 (2021) 108757. https://doi.org/10.1016/j.compscitech.2021.108757.

[29] J.C. Maxwell, A Treatise on Electricity and Magnetism (3rd edition), Clarendon Press, Oxford (1982) (Vol. 1, Chap. 9) 435–441.

[30] D. A. G. Bruggeman, Berechnung verschiedener physikalischer Konstanten von heterogenen Substanzen. I. Dielektrizitätskonstanten und Leitfähigkeiten der Mischkörper aus isotropen Substanzen, Annalen der Physik 416(7) (1935) 636–664.

[31] R. Landauer, The electrical resistance of binary metallic mixtures, Journal of Applied Physics 23(7) (1952) 779–784.

[32] S. Caré, E. Hervé, Application of a n-phase model to the diffusion coefficient of chloride in mortar, Transport in Porous Media 56(2) (2004) 119–135. DOI : 10.1023/B:TIPM.0000021730.34756.40.

[33] R.E.J. Garboczi, K.A. Snyder, J.F. Douglas, M.F. Thorpe, Geometrical percolation threshold of overlapping ellipsoids, Physical Review E 52 (1) (1995) 819–828. https://doi.org/10.1103/PhysRevE.52.819.

[34] Y.B. Yi, A.M. Sastry, Analytical approximation of the percolation threshold for overlapping ellipsoids of revolution, Proceedings of the Royal Society A: Mathematical, Physical and Engineering Sciences 460(2048) (2004) 2353–2380. https://doi.org/10.1098/rspa.2004.1279.

[35] S. Torquato, Y. Jiao, Effect of dimensionality on the percolation threshold of overlapping nonspherical hyperparticles, Physical Review E 87 (2013) Article 022111. 10.1103/PhysRevE.87.022111.

[36] S.H. Jang, D.P. Hochstein, S. Kawashima, H. Yin, Experiments and micromechanical modeling of electrical conductivity of carbon nanotube/cement composites with moisture, Cement and Concrete Composites 77 (2017) 49-59. https://doi.org/10.1016/j.cemconcomp.2016.12.003.

[37] Y.J. Kim, T.S. Shin, H.D. Choi, J.H. Kwon, Y.C. Chung, H.G. Yoon, Electrical conductivity of chemically modified multiwalled carbon nanotube/epoxy composites, Carbon 43(1) (2005) 23-30. https://doi.org/10.1016/j.carbon.2004.08.015.

Appendix: Calculation of volume of three overlapped ellipsoids

The total volume of three overlapped identical ellipsoids shown in Fig.2a can be split into three parts. One is the volume of the inner sphere with radius R_p as shown in Fig.A1. One is the negative volume of six crowns of the sphere as shown in pink colour in Fig.A1. One is the volume of six partial ellipsoids as shown in sky-blue colour in Fig.A1.

Assume the three semi-axes of the ellipsoid are (a, b, b). Thus, the coordinates (x_p, y_p) and the radius R_p of the inner sphere shown in Fig.A1 can be expressed as follows,

$$x_p = y_p = \frac{ab}{\sqrt{a^2+b^2}} = \frac{a}{\sqrt{1+\lambda^2}} \tag{A1}$$

$$R_p = \sqrt{x_p^2 + y_p^2} = \frac{a\sqrt{2}}{\sqrt{1+\lambda^2}} \tag{A2}$$

where $\lambda=a/b$ is the aspect ratio of the ellipsoid. The volume of the inner sphere with radius R_p is calculated as follows,

$$V_1 = \frac{4\pi}{3}R_p^3 = \frac{4\pi a^3}{3}\left(\frac{2}{1+\lambda^2}\right)^{3/2} \tag{A3}$$

The negative volume of six crowns of the inner sphere is calculated as follows,

$$V_2 = -6\pi\left(R_p - x_p\right)^2\left(R_p - \frac{R_p - x_p}{3}\right) = -\frac{(8\sqrt{2}-10)\pi a^3}{(1+\lambda^2)^{3/2}} \tag{A4}$$

The volume of six partial ellipsoids is calculated as follows,

$$V_3 = 6\int_{x_p}^{a} \pi y^2 dx = \frac{2\pi a^3}{\lambda^2}\left(2 - \frac{3x_p}{a} + \frac{x_p^3}{a^3}\right) = \frac{2\pi a^3}{\lambda^2}\left(2 - \frac{3}{\sqrt{1+\lambda^2}} + \frac{1}{(1+\lambda^2)^{3/2}}\right) \tag{A5}$$

Hence, the volume of the three overlapped ellipsoids is expressed as,

$$\Omega_{in}(\lambda, a) = V_1 + V_2 + V_3 = \frac{4\pi a^3}{\sqrt{(1+\lambda^2)^3}}\left(\frac{3-4\sqrt{2}}{3} + \frac{\sqrt{(1+\lambda^2)^3}-1}{\lambda^2}\right) \tag{A6}$$

As expected, Eq.(A6) gives $\Omega_{in}=4\pi a^3/3$ if $\lambda=1$. Also, it is indicated that if $\lambda\to\infty$ then $\Omega_{in}\to 0$. The former represents the spherical inclusions; whereas the latter stands for the line inclusions of infinite small cross-section.

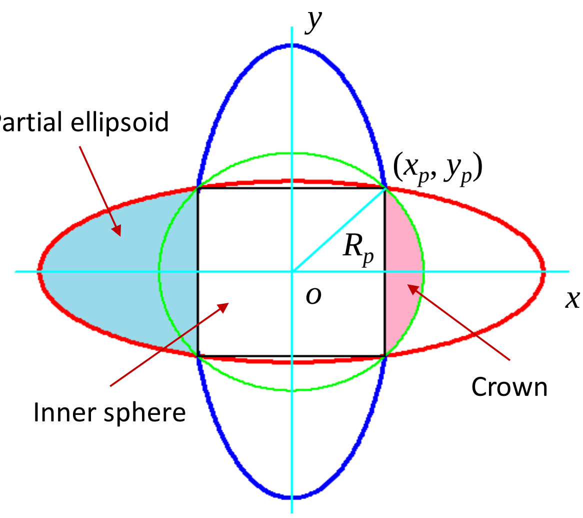

Fig.A1 Plan view of object of overlapped ellipsoids with semi-axes of (a, b, b).